

18  
6-14-95 50

LBL-36831  
UC-400



# Lawrence Berkeley Laboratory

UNIVERSITY OF CALIFORNIA

## EARTH SCIENCES DIVISION

### **Discriminating Effects of Heterogeneity and Matrix Diffusion by Alternative Tracer Designs**

Y.Y.W. Tsang

March 1995



DISTRIBUTION OF THIS DOCUMENT IS UNLIMITED

Prepared for the U.S. Department of Energy under Contract Number DE-AC03-76SF00098

#### DISCLAIMER

This document was prepared as an account of work sponsored by the United States Government. While this document is believed to contain correct information, neither the United States Government nor any agency thereof, nor The Regents of the University of California, nor any of their employees, makes any warranty, express or implied, or assumes any legal responsibility for the accuracy, completeness, or usefulness of any information, apparatus, product, or process disclosed, or represents that its use would not infringe privately owned rights. Reference herein to any specific commercial product, process, or service by its trade name, trademark, manufacturer, or otherwise, does not necessarily constitute or imply its endorsement, recommendation, or favoring by the United States Government or any agency thereof, or The Regents of the University of California. The views and opinions of authors expressed herein do not necessarily state or reflect those of the United States Government or any agency thereof, or The Regents of the University of California.

Available to DOE and DOE Contractors  
from the Office of Scientific and Technical Information  
P.O. Box 62, Oak Ridge, TN 37831  
Prices available from (615) 576-8401

Available to the public from the  
National Technical Information Service  
U.S. Department of Commerce  
5285 Port Royal Road, Springfield, VA 22161

Lawrence Berkeley Laboratory is an equal opportunity employer.

## **DISCLAIMER**

**Portions of this document may be illegible in electronic image products. Images are produced from the best available original document.**



LBL-36831  
UC-400

**Discriminating Effects of Heterogeneity and Matrix  
Diffusion by Alternative Tracer Designs**

Yvonne Y.W. Tsang

Earth Sciences Division  
Lawrence Berkeley Laboratory  
University of California  
Berkeley, California 94720

March 1995

This work was jointly supported by Sandia National Laboratories, WIPP Project Office under Contract No. DE-AC04-94A185000, and by the Power Reactor and Nuclear Fuel Development Corporation (PNC), Tokyo, Japan, through the U.S. Department of Energy under Contract No. DE-AC03-76SF00098.

DISTRIBUTION OF THIS DOCUMENT IS UNLIMITED

**MASTER** *for*

# Discriminating Effects of Heterogeneity and Matrix Diffusion by Alternative Tracer Test Designs

Y. W. Tsang

*Earth Sciences Division, Lawrence Berkeley Laboratory,  
University of California, Berkeley, California*

## ABSTRACT

Flow and transport calculations are carried out by numerical simulation for different tracer designs: single-well radially diverging/converging (huff-puff), single well radially converging, and two-well injection-withdrawal (doublet) in a 2D fracture zone. The fractured rocks are conceptualized as a dual-continuum: the well-connected fractures forming a heterogeneous continuum for advective transport, and the less permeable matrix forming a second continuum for tracer diffusion. Results show that the huff-puff design can be a good diagnostic test for matrix diffusion. The two-well doublet design averages over a large volume and corrects for the extreme sensitivity to spatial heterogeneities of the single well converging test, but requires prior knowledge of presence or absence of matrix diffusion to give reliable estimate of transport parameters. Results of this study demonstrate that using a suite of different tracer designs is important to reduce the uncertainty in association with solving the inverse problem of tracer test interpretation to characterize transport in fracture rocks.

## INTRODUCTION

The inverse problem of deducing parameters which characterize transport in geological formations from tracer test data is inherently non-unique; that is, equally good fit to the tracer test data may be obtained from different conceptual models and their associated parameters. For example, breakthrough curves for transport in a heterogeneous fractured medium often have the characteristics of a fast rise and a long tail (Frost and Davison, 1994; Gustafsson and Nordqvist, 1993). But this fast rise and long tail in the tracer breakthrough can also be ascribed to retardation processes such as matrix diffusion, or to well bore effects at the tracer injection or sampling wells (e.g. Novakowski, 1992). Since interpretation of tracer data usually does not end at data fitting, rather the results are used for prediction, or up scaling; then it is crucial to minimize the model uncertainty, and to maximize confidence in the "correctness" of the conceptual model employed.

In this paper we explore the role of different tracer test designs to discriminate different processes which affect the transport, thus aid in reducing model uncertainty. We place emphasis on the interference of heterogeneity with matrix diffusion, and its effect on the inverse problem. The test designs studied are: single well radially diverging-converging flow (huff-puff), single well radially converging flow, and two well injection-withdrawal flow (doublet). Gelhar et al. (1992) discussed the effects of different tracer designs on the reliability of the reported dispersivity in a critical review of published field-scale dispersion from tracer experiments. They maintain that in huff-puff tests the dispersion is reversed at the pumping phase, hence is unsuitable for determination of medium dispersivity. Our study shows that for the same reason that huff-puff design underestimates dispersivity due to

heterogeneity, it proves to be particularly effective in determining matrix diffusion parameters.

## APPROACH

Fracture media can be conceptualized either as a discrete network, where connectivity is very much an issue, or as a continuum. In this paper we conceptualize a fracture zone as a 2D dual-continuum. The fractures in the fracture zone are expected to have a high enough density and be connected enough to be well approximated by a heterogeneous stochastic continuum for advective transport. The low permeability “matrix” between fractures forms a second continuum which contributes negligibly to the advective transport, but participates in the exchange of tracer with the fractures by diffusion. Flow and transport calculations in the fracture zone are carried out by numerical simulation. Numerical simulation is the method chosen here because analytical solutions for dual-continuum transport for different radial flow configuration in 2D are not available for a heterogeneous medium. Welty and Gelhar (1994) give analytical solutions for the common radial single well and two well tracer-test designs within the single continuum approximation in which matrix diffusion is absent. Their solutions are valid in the limit of Fickian dispersion, that is, when dispersivity due to heterogeneity is much less than 1/10 of the test scale.

### Generation of Stochastic Hydraulic Conductivity Fields in 2D

Mathematically, the heterogeneous fracture continuum is represented by a 2D stochastic field of hydraulic conductivity. The turning band method (Tompson et al, 1989) is used for the generation of a lognormal field specified by a mean and a variance  $\sigma^2$  in  $\ln K$ . The permeabilities are correlated with an exponential covariance:

$$C(\zeta) = \sigma^2 \exp\left\{-\left[\left(\frac{\zeta_1}{a_1}\right)^2 + \left(\frac{\zeta_2}{a_2}\right)^2\right]\right\}^{1/2} \quad (1)$$

where  $\zeta$  is the separation vector and  $a$  is the anisotropic correlation parameter. For this study, an isotropic correlation structure is assumed, hence  $a_1=a_2=a$ . Because of the slow decay of the exponential function, permeabilities within a domain of several  $a$ 's are expected to be correlated, hence one may consider the characteristic scale of the heterogeneous stochastic field  $\lambda$  to be around  $3a$ . It is recognized in the research community that spatial heterogeneity occurs at all scales in geologic formations, and that the relevant scale of heterogeneity which will introduce observable effects in measurements is that scale which is comparable in order of magnitude to the measuring scale. For heterogeneities which are of a much smaller scale than the measurement, their effects will be averaged out and are manifested in a value of the macrodispersivity being  $< 1/10$  of the test scale. For heterogeneities which are of a much larger scale than the measurement, they will be “invisible” to the measurement in that the results resemble that of a homogeneous medium since the entire measurement domain lies within the much larger heterogeneities. Therefore the heterogeneities which are likely to give transport results significantly different from that of a homogeneous medium would be those with correlation scale  $\lambda$  of perhaps  $1/5$  to  $1/2$  of the measurement region. The fact that flow channeling is so often observed in tracer experiments in the field (e.g. Gustafsson and Nordqvist, 1993; Frost and Davison, 1994) indicates that the correlation scale of

heterogeneity on the order of test scale (dispersivity  $>1/10$ ) is often in operation in the field. For if the dispersivity due to heterogeneity is much less, the tracer results should reflect the properties of a homogeneous medium. In order to specifically include the effects of heterogeneity, in all our numerical studies the correlation scale  $\lambda$  of the stochastic heterogeneous hydraulic conductivity,  $K$ , is chosen to be about  $1/5$  to  $1/3$  of the test scale.

### Flow and Transport Calculations

Steady state flow calculations are carried out for different flow fields for the common tracer test designs (Figure 1). Figure 1 shows schematically the boundary conditions for the flow simulation. The dark shaded region is the fracture zone mathematically represented by a stochastic field of hydraulic conductivity geostatistically generated by the turning band method (Tompson et al., 1989). The thick dark lines represent closed boundaries. The constant head ( $H_1$  and  $H_2$ ) boundaries in the huff-puff design allow a regional drift velocity as well as the radial flow field from the center injection and pumping well. The heterogeneous field domain is chosen to be about three times that of the maximum extent of the plume size to minimize effect of the boundary on the calculations. For the doublet configuration the flow field is taken to be several times that of the stochastic field (dark shaded) region. The lightly shaded region surrounding the stochastic field is given coarser grids and a uniform hydraulic conductivity identical to the geometric mean of the stochastic hydraulic conductivity. For the single well converging test all nodes beyond a radial distance (with respect to the pumping well) are given an uniform hydraulic conductivity ten times that of the largest conductivity in the field, in order to insure that the constant head ( $H$ ) boundaries applied on the square region is transmitted to the radial boundary.

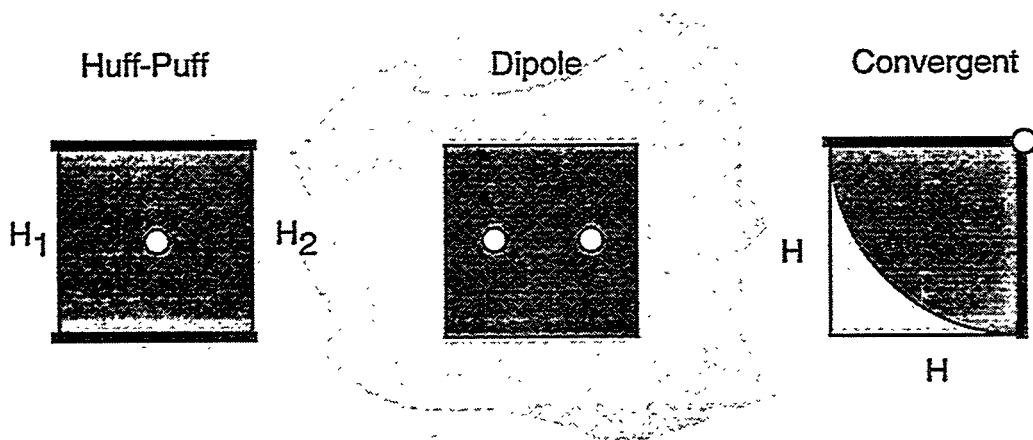


**Figure 1** Schematic diagram of respective boundary conditions for calculating flow and transport for different tracer configurations.

For flow calculations, the heterogeneous domain is discretized into  $180 \times 180$  elements with dimensions  $\Delta x$ ,  $\Delta y$ ; and for each node  $i$ , other than the node(s) of the injection and/or withdrawal well(s), mass balance for steady state flow would prescribe that:

$$\sum_j Q_{ij} = \sum_j K_{ij} A_{ij} (H_i - H_j) = 0 \quad (2)$$

where  $Q_{ij}$  is the volumetric flow from node  $i$  to  $j$ ,  $K_{ij}$  is the hydraulic conductivity, and  $A_{ij}$  is the interfacial area between nodes  $i$  and  $j$ . For the node(s) of the injection and withdrawal wells, the right hand side of Equation 2 will respectively be the injection rate (+) or the withdrawal rate (-), as appropriate for the different tracer designs. Except for the nodes at the boundaries where the hydraulic heads are prescribed, the hydraulic heads  $H_i$  are unknowns. The system of Equations (2) is solved using a conjugate gradient iterative solver. Then the steady state volumetric flow  $Q_{ij}$  and the steady state velocity  $v_{ij}=Q_{ij}/A_{ij}$  from node  $i$  to  $j$  are calculated. In this way the steady state flow field for a heterogeneous fracture zone is obtained for the respective tracer design.

After the steady state flow field is obtained, transient advective transport in the fracture heterogeneous continuum is simulated by particle tracking method (Moreno et al., 1988) with matrix diffusion incorporated (Yamashita and Kimura, 1990; Moreno and Neretnieks, 1993). A large number of particles are introduced in the injection well during the introduction of the tracer slug. In the single-continuum mode of transport, the residence time  $t_w$  for the particle to reside within each discretized element is determined from the pore volume of the fracture continuum divided by the amount of flow that passes through it:

$$t_w = \frac{h\phi_f \Delta x \Delta y}{\frac{1}{2} \sum_j |Q_{ij}|} \quad (3)$$

where  $h$  is the thickness of the fracture zone and  $\phi_f$  is the porosity of the fracture continuum. Each particle is moved along in the respective flow fields and the residence times within the different discretized elements along its path are summed. At each intersection of four nodes, tracer particles are distributed in the outlet branches according to steady state stream tubes and they are also assumed not to diffuse across these stream tubes, that is, a no mixing approximation is implemented at the intersections (Moreno et al., 1990).

Equation 3 for the residence time in a given discretized element will be modified in the dual-continuum mode of transport when diffusion into the matrix continuum is allowed. For an idealized parallel plate fracture of length  $L$ , width  $W$ , and aperture  $\delta$ , and for a 1D steady state volumetric flow rate of  $Q$  through the fracture, the advective residence time for plug flow in the fracture is  $t_w = LW\delta/Q$ , so that the tracer breakthrough at the fracture outlet is a step function at  $t=t_w$ . For such an idealized fracture from which matrix diffusion is linear and perpendicular to the fracture surface, an analytical solution (Neretnieks, 1980) is available for the residence time distribution of the solute concentration at the fracture outlet:

$$\frac{C}{C_0} = \text{erfc} \left( \frac{(k_d \rho_p D_e)^{1/2} t_w}{(t - t_w)^{1/2} \delta} \right) \quad (4)$$

The parameters in Equation (4) are  $D_e$ , the effective water diffusion coefficient in the matrix pores,  $k_d$ , the sorption coefficient and  $\rho_p$ , the matrix rock density. For non-sorbing tracer,  $k_d\rho_p$  is simply the matrix porosity  $\phi_m$ . Only non-sorbing tracer is considered in this study. To incorporate effects of matrix diffusion into particle tracking a number is drawn randomly from the uniform distribution  $R[0,1]$ , then the travel time  $t$  for each particle in an element  $i$  (with plug flow residence time  $t_w$ ) is inversely calculated from equation (4). The inverse calculation for  $t$  for a random sample of values from  $R[0,1] = C/C_0$  is illustrated in Figure 2. Our implementation of matrix diffusion into the particle tracking scheme was verified against an analytical solution for 1D transport (Tang et al., 1981):

$$\frac{C}{C_0} = \operatorname{erfc} \left[ \frac{z\sqrt{D_e\phi_m}}{v^{1/2}(vt-z)^{1/2}\delta} \right] \quad (5)$$

where  $C/C_0$  is the distribution of mass concentration along the fracture length  $z$  for constant transport velocity of  $v$  at time  $t$ .

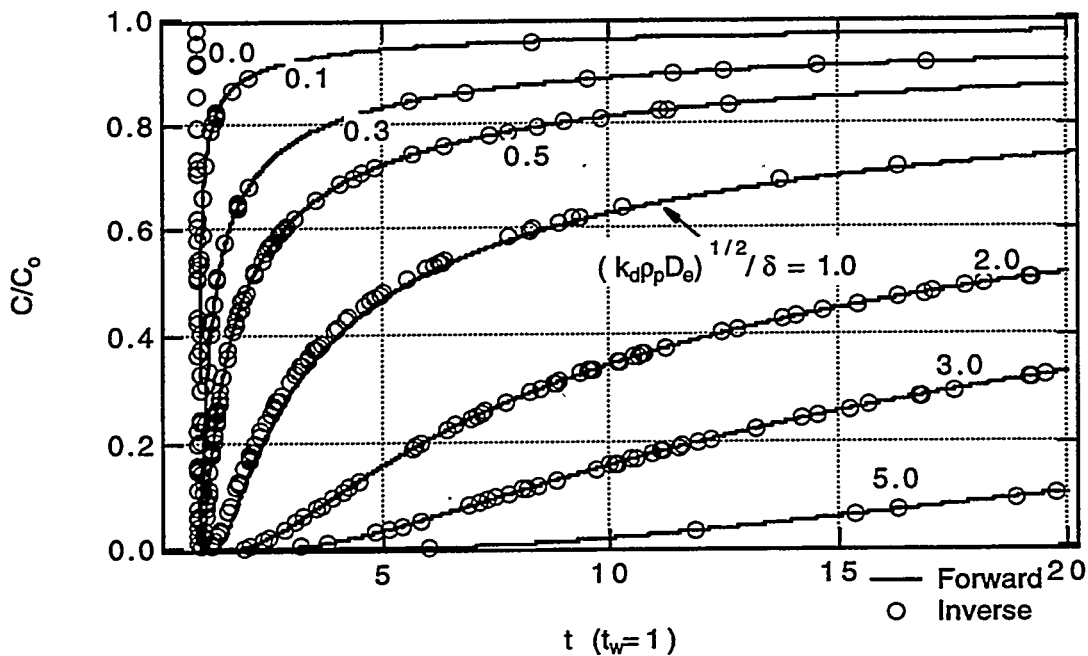


**Figure 2** Inverse calculation of the particle residence time in the fractured-porous medium for the analytical solution of Equation 4 with different values of the parameter group  $(K_d\rho_p D_e)^{1/2}/\delta$ .

Throughout the study, calculations are also carried out for the homogenous case by imposing an uniform hydraulic conductivity to the flow domain. Calculation parameters for all cases studied are summarized in Table 1. The formation parameters are based on the conditions in the Culebra dolomite at the WIPP site in southeastern New Mexico.

**Table 1 Calculation Parameter values**

Fracture zone thickness, h	7.6m
Heterogeneous field domain	60 - 90 m
Injection/withdrawal rates for huff-puff test	$.158 \times 10^{-3} \text{ m}^3/\text{s}$
Transport distance, converging test	30m
Two well separation in doublet test	30m
Pumping rates, converging and doublet tests	$1. \times 10^{-3} \text{ m}^3/\text{s}$
Mean hydraulic conductivity K for fracture zone	$4.47 \times 10^{-6} \text{ m/s}$
Standard deviation $\sigma$ in $\ln K$ ,	1.73, 3.46
Characteristic correlation scale of heterogeneity $\lambda=3a$ for huff-puff test	2.2 m
Characteristic correlation scale $\lambda=3a$ for converging and doublet tests	5.94 m
Fracture continuum porosity, $\phi_f$	0.001
Linear fracture spacing or matrix block size for matrix diffusion, l	0.2 m
Fracture aperture $\delta$ in Eqs (3) and (4), deduced from $3\delta / l = \phi_f$	67 $\mu\text{m}$
Matrix porosity, $\phi_m$	0.16
Matrix tortuosity, $\tau$	0.11
Free water diffusion coefficient, D	$7.4 \times 10^{-10} \text{ m}^2/\text{s}$
Effective matrix diffusion coefficient, $D_e = D\phi_m\tau$	$1.3 \times 10^{-11} \text{ m}^2/\text{s}$

## RESULTS

### Single Well Diverging/Converging (Huff-Puff) Tracer Test

Simulations were carried out for both the single- and dual- continuum descriptions of the fracture-matrix system. Figure 3a shows the plume spatial extent at the end of a 5-hour injection period for a tracer slug introduced in the first 100 minutes of injection, for a homogeneous field and single-continuum representation where matrix diffusion is absent. The plume is a ring 20 m in diameter and centered on the injection well. The radial symmetry for flow in the homogeneous field is evident. Figure 3b shows the plume spatial extent at the end of the same 5-hour injection period for a moderately heterogeneous hydraulic conductivity field and single-continuum simulation. Here in Figure 3b the radial symmetry is masked by flow channeling effects arising from small scale heterogeneities of the fracture continuum.

The rate of mass recovery (which is proportional to tracer concentration when the flow rate is constant) versus time for different cases studied are shown in Figure 4. On each Figure (4a and 4b) is shown results for four cases: homogeneous and heterogeneous, single continuum and dual-continuum. In the single-continuum case, flow channeling due to heterogeneity gives rise to considerable tailing as compared to the homogeneous results. On the other hand, in the dual-continuum model, matrix diffusion gives rise to even longer tail in

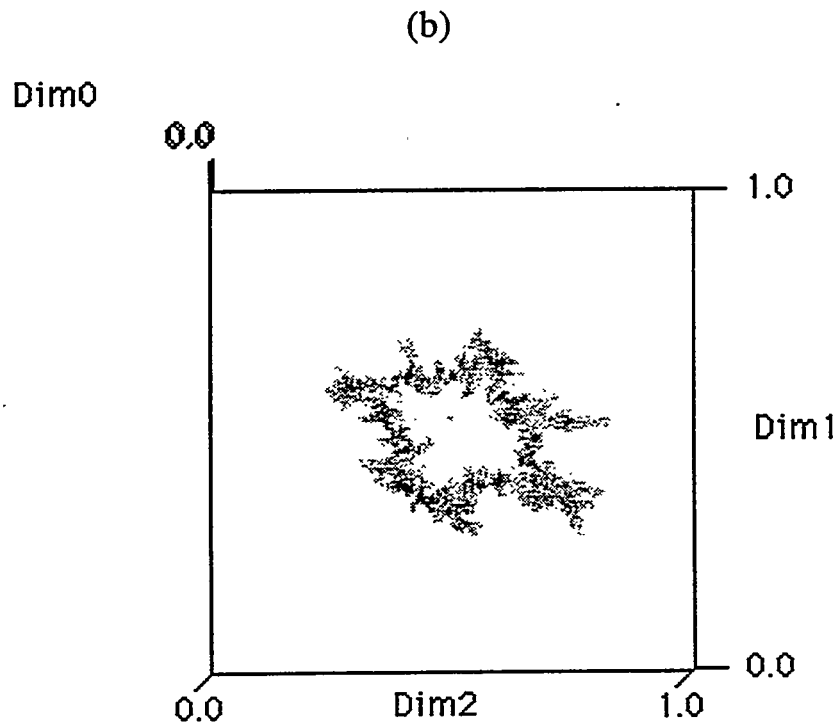
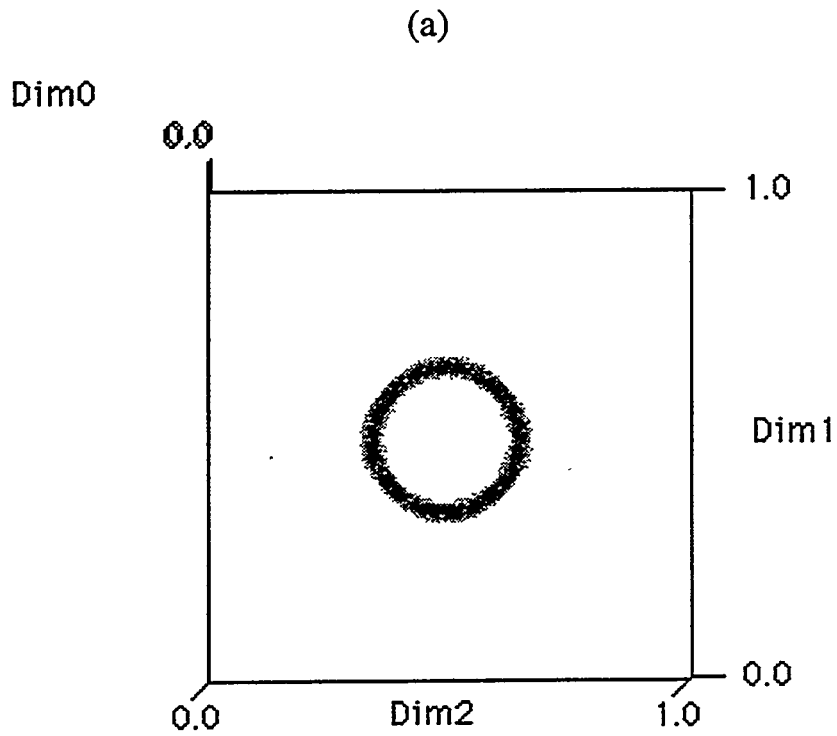


**Figure 3** The spatial plume distribution for the first 100 minutes tracer slug at the end of a 5-hour injection period, for single-continuum transport in (a) a homogeneous continuum and (b) a moderately heterogeneous fracture continuum ( $\sigma_{\ln K}=1.73$ ).

both the homogeneous and the heterogeneous results with a similar  $-3/2$  slope on a log-log plot. This  $-3/2$  slope arises from the asymptotic  $t^{3/2}$  dependence in the analytic solution for dual-continuum tracer transport (Konosavsky et al., 1993). Figure 4b shows the results for an extremely heterogeneous field where the standard deviation of hydraulic conductivity  $\sigma_{\ln K}$  is 3.46, doubling that of the heterogeneous field for Figure 4a. It is evident that the severe flow channeling here yields a long tail with a greatly reduced negative slope for the extreme heterogeneous field in the single continuum simulation. Yet the effect is still not large enough to confuse it with the dual-continuum results, where the asymptotic time dependence of  $t^{3/2}$  is evident for both the strongly heterogeneous and the homogeneous descriptions of the 2D fracture zone.

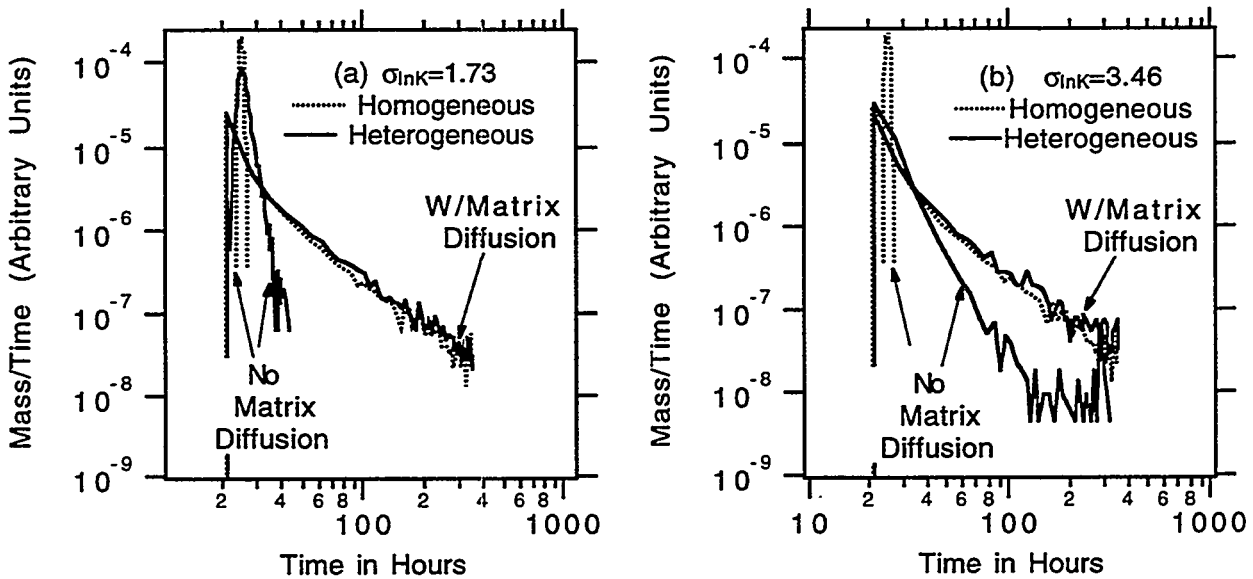


**Figure 4** Diverging/converging (huff-puff) tracer recovery curves for the single- and dual-continuum representations of the homogeneous and heterogeneous fractured zone, (a)  $\sigma_{\ln K} = 1.73$  and (b)  $\sigma_{\ln K} = 3.46$ .

### Single Well Radially Converging Test

Flow calculations are carried out for the single well convergent test configuration. Figure 5 shows the flow field for a particular realization of a heterogeneous fracture zone with the pumping well located at the top right corner of the heterogeneous field. The magnitude of the flow increases with the darkness of the gray scale, clearly illustrating the presence of flow channeling. For each steady state flow field, transient transport calculations

by particle tracking are carried out for nine equally spaced positions of the injection well on a radius of 30 m from the pumping well. While tracer recovery curves are invariant with the position of the injection wells for homogeneous fields, they will differ with the position of injection well in a heterogeneous field due to channeling as illustrated in Figure 5. The fastest and the slowest tracer arrival among the nine injection well results will be selected to be displayed in tracer breakthrough curves in Figure 6.

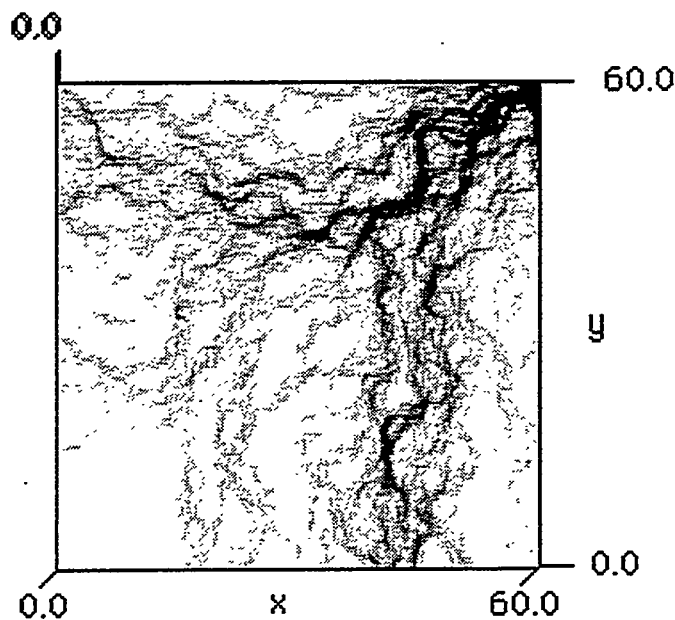


**Figure 5** Flow field in the converging configuration in a heterogeneous ( $\sigma_{\ln K}=1.73$ ) fracture zone.

In Figure 6 the tracer recovery curves at the pumping well are shown. The results for the single continuum (no matrix diffusion) conceptual model are in solid lines, and the results for the dual continuum (with matrix diffusion) conceptual model are in dotted lines. For the homogeneous medium, one breakthrough curves is shown for the single-continuum conceptual model, and one for the dual-continuum conceptual model. For the heterogeneous medium, two recovery curves, the earliest and latest arrival of the nine injection cases, are displayed respectively for the single- and dual-continuum models. Figure 6a shows results for a heterogeneous continuum with  $\sigma_{\ln K}=1.73$ , and Figure 6b for an extreme heterogeneous medium where  $\sigma_{\ln K}$  is 3.46. All plots are on log-log scale. It is evident that for a homogeneous continuum the presence of matrix diffusion with the characteristic  $-3/2$  slope is

clearly distinguishable from the single continuum model which has a  $-\infty$  slope. However, for heterogeneous fields, particularly for large  $\sigma$  in Figure 6b, distinction between the results for single- and dual-continuum begins to blur. This means that without an independent means to ascertain the presence of matrix diffusion, tracer data may be interpreted with either a single- or dual-continuum description, leading to very different predictions of transport parameters such as porosity and dispersion. Furthermore, that the tracer arrival times varies widely for different injection well location underlines that, even if the correct conceptual model is used to account for the processes of transport, great uncertainty remains in the deduced parameters because of the sensitivity of results to spatial variability in the fractured zone.

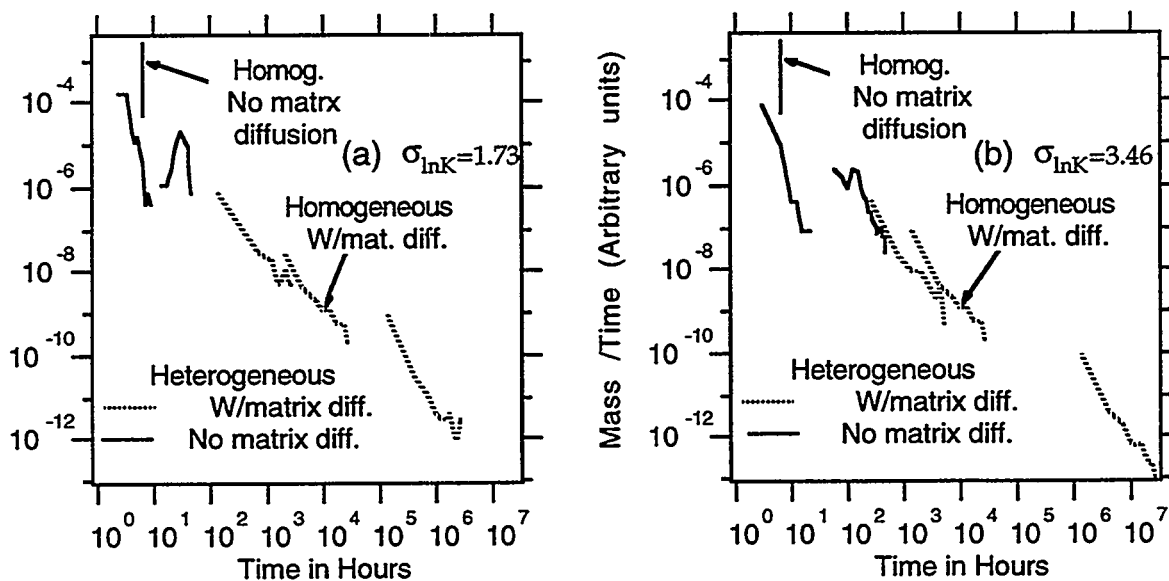


**Figure 6** Single well converging tracer recovery curves in the single- and dual-continuum models of the homogeneous and heterogeneous fractured zone (a)  $\sigma_{\ln K} = 1.73$  and (b)  $\sigma_{\ln K} = 3.46$ .

### Two Well Injection-Withdrawal (Doublet) Tracer Test

Figure 7 shows the flow field in a heterogeneous fracture zone for a doublet tracer test configuration. The injection and withdrawal wells are positioned at 405 m on the y axis and 390 m and 420 m respectively on the x axis. The injection and withdrawal flow rates are equal. We note that the steady state flow stream lines are distorted from the pattern of regular dipole stream lines because of heterogeneity. In this doublet test configuration the tracer recovery curves at the withdrawal well include transport which covers a large flow region, that is, the tracer recovery curves involve a large amount of spatial averaging, as opposed to the tracer recovery curves for the previously discussed radially converging tracer test. The spatial

averaging may therefore give a better estimate of the transport parameters which characterize the fracture zone.

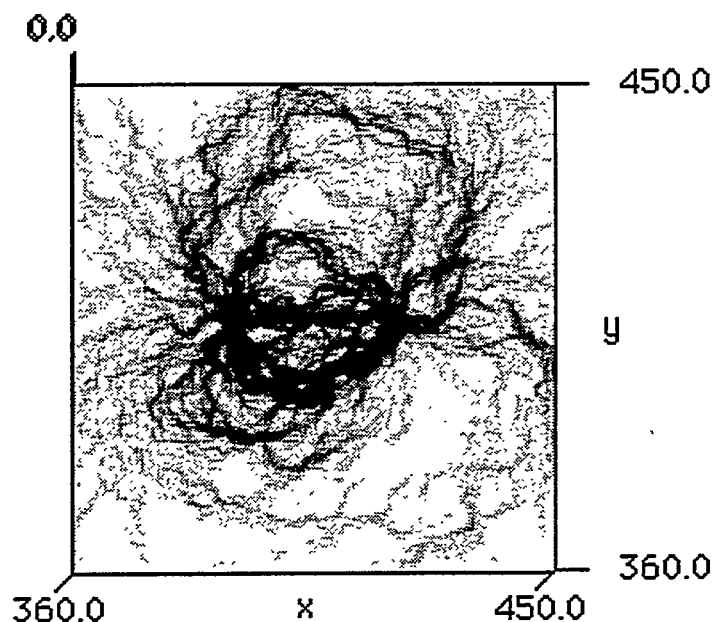


**Figure 7** Flow field for the two-well doublet configuration in a heterogeneous ( $\sigma_{\ln K}=1.73$ ) fracture zone.

Figure 8 shows the tracer recovery curves for both homogeneous and heterogeneous fields, and for single- and dual- continuum descriptions. The solid lines denote the heterogeneous results, and the dotted lines denote the homogeneous results. The striking feature in Figure 8 is that both the single- and dual- continuum models give similar negative slope in the log-log plot, though the arrival time differs by several orders of magnitude, with the matrix diffusion effects giving rise to very large time delay. Within the same conceptual model, either the single- or dual- continuum description, homogeneous and heterogeneous results are also similar. Therefore the spatial averaging in the doublet design is indeed effective in minimizing the observable effects of flow channeling due to heterogeneity in the tracer results. The doublet tracer design therefore corrects for the sensitivity to spatial variability encountered in the converging test (Figure 6).

An examination of the analytical solution for doublet configuration for a single-continuum shows that the asymptotic slope of the tracer recovery on a log-log plot is very close to  $-3/2$ ; the very long tail arises purely from the large range of path lengths in the doublet configuration. Therefore the asymptotic behavior of  $t^{-3/2}$  characteristic of matrix diffusion in single well radial flow geometry is no longer distinct from its absence in the doublet design. There is now in the doublet configuration no clear signature for the presence of matrix diffusion at any level of heterogeneity, though matrix diffusion has the effect of shifting the arrival time by orders of magnitude. This implies that estimation of site

characterization parameters can involve large uncertainty unless prior knowledge of presence or absence of matrix diffusion exists.

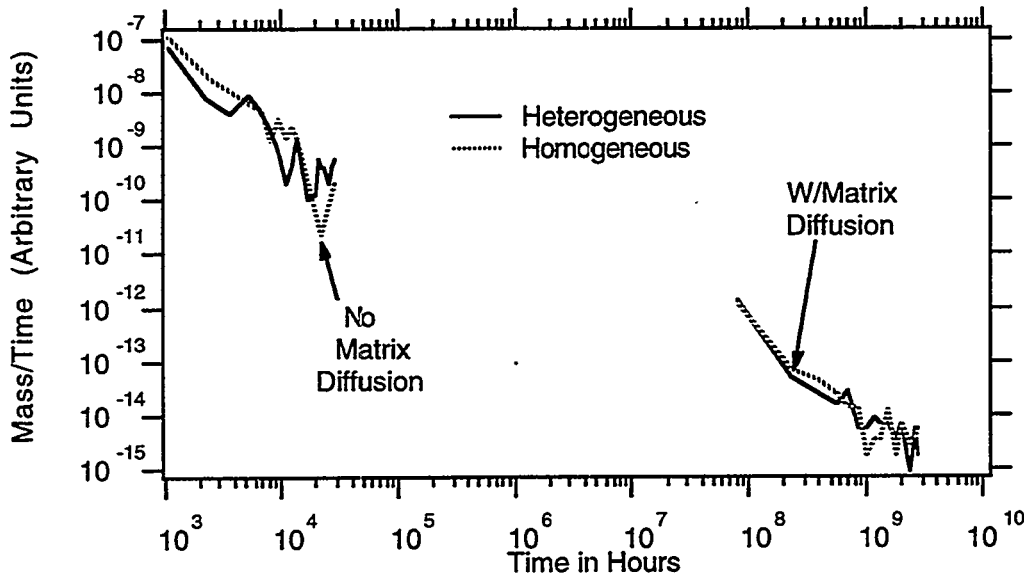


**Figure 8** Tracer recovery curves for doublet in the single- and dual- continuum representations of the homogeneous and heterogeneous ( $\sigma_{\ln K}=1.73$ ) fields.

## CONCLUSION

The above results illustrate that different tracer test designs place emphasis on different aspects of the transport process in a fractured zone. Testing with more than one design can reduce both the conceptual model and parameter uncertainty. The huff-puff test seems particularly suited as a diagnostic test to ascertain the presence of matrix diffusion in the field. Even extreme heterogeneity fails to drown out the characteristic asymptotic  $t^{-3/2}$  signature of the dual-continuum tracer recovery. It is a good first test to either rule out the presence of matrix diffusion, or to deduce the matrix diffusion parameter group. If matrix diffusion is in operation, then the peak concentration for the tracer recovery would decline with the resting period imposed between injection and withdrawal. This relationship can be used to calibrate the matrix diffusion parameter group. However, since multiple mixing processes are usually present in the field, confirmatory determination of matrix diffusion in the laboratory is recommended.

In addition to inherent tracer test uncertainty such as incomplete flushing of the source term, the converging test results are also particularly sensitive to spatial heterogeneity in that the recovery curve can vary greatly with the position of the injection well in a fracture zone. The spatial variability of tracer breakthrough is to be expected from "point" measurements. The doublet tracer test configuration on the other hand involves a special spatial averaging of flow paths and corrects for the extreme spatial variability of "point" measurements. However, the dispersion due to the broad range of doublet path lengths has

similar characteristics as dispersion due to retardation by matrix diffusion. Therefore, the doublet test design yields "average" fracture porosity more representative of a fractured zone only if prior knowledge exists as to the appropriateness of either the single- or dual-continuum model. Otherwise though the spatial variability is reduced by the doublet configuration, yet the model uncertainty is increased by the same choice of two-well configuration.

In conclusion, this study demonstrates that a suite of different tracer designs can reduce the uncertainty in the interpretation of the tracer data to characterize the transport properties of a 2D heterogeneous fractured zone.

#### ACKNOWLEDGMENT

The author thanks C. F. Tsang and J. Wang of LBL for review and comments on the manuscript. Assistance from S. Nachnani in computing and graphics is gratefully acknowledged. This work was jointly supported by Sandia National Laboratories, WIPP Project Office, and by the Power Reactor and Nuclear Fuel Development Corporation (PNC), Tokyo, Japan, through U.S. Department of Energy Contract No. DE-AC03-76SF00098.

#### REFERENCES

- Frost, L.H. , C.C. Davison, Summary of the fracture zone 3 groundwater tracer test program at the underground research laboratory. *AECL Technical Record Report TR-617*, 69 pp., Atomic Energy of Canada Limited, Pinawa, Manitoba, Canada, 1994.
- Gustafsson, E., R. Nordqvist, Radially converging tracer test in a low-angle fracture zone at the Finnsjöhn site, central Sweden, *SKB Technical Report TR 93-25*, Swedish Nuclear Fuel and Waste Management Co., Stockholm, Sweden, 1993.
- Gelhar, L.W., C. Welty, K.R. Rehfeldt, A critical review of data on field-scale dispersion in aquifers. *Water Resour. Res.*, 28(7), 1955-1974, 1992.
- Konosavsky, P., V. Mironenko , V. Rumynin, Development and reexamination of models of tracer tests for fractured reservoirs, *Geoecology*, Russian Academy of Sciences, 104-124, 1993.
- Moreno, L., Y.W. Tsang, C.F. Tsang, F.V. Hale, I. Neretnieks, Flow and tracer transport in a single fracture: A stochastic model and its relation to some field observations, *Water Resour. Res.*, 24(12), 2033-2048, 1988.
- Moreno, L., C. F. Tsang, Y.W. Tsang, I Neretnieks, Some anomalous features of flow and solute transport arising from fracture aperture variability, *Water Resour. Res.*, 26(10), 2377-2391, 1990.
- Moreno, L., I. Neretnieks, Fluid flow and solute transport in a network of channels, *J. Cont. Hydrology*, 14, 163-192, 1993.
- Neretnieks, I., Diffusion in the rock matrix: An important factor in radionuclide retardation? *J. Geophys. Res.*, 85 (B8), 4379-4397, 1980.
- Tang, D. H., E.O. Frind and E. A. Sudicky, Contaminant transport in fracture porous media; Analytical solution for a single fracture, *Water Resour. Res.*, 17(3), 555-564, 1981.
- Tompson, A. F. B., R. Ababou, L. W. Gelhar, Implementation of the three-dimensional turning bands random field generator, *Water Resour. Res.*, 25(10), 2227, 2243, 1989.
- Welty,C., L.W. Gelhar, Evaluation of longitudinal dispersivity from non uniform flow tracer tests, *J. of Hydrology*, 153, 71-102, 1994.

Yamashita, R., H. Kimura, Particle-tracking technique for nuclide decay chain transport in fractured porous media, *Journal of Nuclear Science and Technology*, 27, 1041-1049, 1990.